

**Fine Structure of the Spermatozoon in the Japanese
Abalone, *Haliotis discus***

Yoko Shiroya and Yoshi T. Sakai

Biological Laboratory, Wayo Women's University,
Ichikawa, Chiba 272

ABSTRACT

Spermatozoa of *Haliotis discus* were subjected to observations by light and electron microscopies. A differential interference microscope as well as a dark-field microscope was capable of distinguishing the acrosome from the nucleus. Observations of the live spermatozoa by the light microscopies confirmed in detail the overall figures of the sperm head observed by scanning or transmission electron microscopy. The acrosomal vesicle showing a length of 2.8 μm and a diameter of 1.1 μm contained two kinds of materials different in electron density. Around the apex of the acrosome, a trigger region of the acrosome reaction and a structure termed truncated cone were visible. The axial rod was shown to penetrate deeply into both the acrosomal vesicle and the nucleus in the opposite directions. The boundary between the acrosome and the nucleus exhibited a diamond-shaped region with the axial rod through it. The midpiece was composed of five mitochondria and a pair of centrioles being oriented orthogonally in the center of the midpiece. The proximal centriole was placed in a depression of nucleus at the posterior end and the distal centriole was associated with nine spokes, which connected the centriole with the mitochondria.

INTRODUCTION

Fertilization is usually proceeded by the acrosome reaction that occurs when the spermatozoon reaches the protective coat surrounding the egg (1). The reaction is comprised of two important steps: one is the release of membrane lysin for dissolution of the egg envelope, and the other is the formation of the acrosomal process composed of a bundle of microfilaments.

Concerning the acrosomal process, earlier studies indicate that some of the mature spermatozoa have only the precursor materials as in echinoderms and the acrosomal process is formed from these materials during the acrosome reaction. In *Neanthes* and *Mytilus*, on the other hand, the spermatozoa possess preformed filamentous bundle termed axial rod that grows longer during the acrosome reaction (2,3).

In molluscan spermatozoa, the bivalves, *Barnea* and *Crassostrea*, are known to have only the fibrous precursor different from *Mytilus* spermatozoon (4,5). However, our preliminary observations show that the spermatozoa of snails, *Tegula* and *Turbo*, possess the axial rod as does *Mytilus* spermatozoon. These molluscan spermatozoa generally have large acrosomes and therefore favor studies of the structure of the acrosome and the mechanism of the acrosome reaction.

The structure of the abalone spermatozoon, *Haliotis rufescens*, has recently been described by Lewis et al. (6). Using the Japanese abalone, *Haliotis discus*, we have found that remarkable changes occur in the acrosome during the acrosome reaction (7). However, the process and mechanism of the formation of the acrosomal process are still unknown. For clarifying the problems, it is requisite to visualize the fine structures of the abalone sperm in more detail. The abalone spermatozoon has so large an acrosome that it is easily distinguishable from the nucleus even under the light microscope. This facilitates comparison of microscopic figures observed by light and electron microscopies.

This paper deals with morphological comparison of

the abalone spermatozoa using scanning and transmission electron microscopes as well as differential interference and other light microscopes. Further observations of the fine structures are also given in more detail.

MATERIALS AND METHODS

Mature shells of Japanese abalone, *Haliotis discus*, were provided by the Chiba and Kanagawa Prefectural Fisheries Experimental Stations.

Gametes were induced to spawn by exposing mature shells into UV-irradiated sea water according to the method of Kikuchi and Uki (8). Mass of the sperm just spouting up from the spawning hole was collected using a pipette with a minimal amount of sea water.

The intact spermatozoa were subjected to observation using a Nomarski differential interference microscope or a dark-field microscope equipped with a mercury arc lamp.

For scanning or transmission electron microscopy, the spermatozoa were fixed with 1% OsO_4 in 0.1 M sodium phosphate buffer (pH 7.4), or with 2.5% glutaraldehyde in 0.1 M sodium phosphate buffer (pH 7.4) and postfixed with 1% OsO_4 . The fixed material was washed with 0.1 M sodium phosphate buffer (pH 7.4) and dehydrated in a graded series of ethanol. Specimens for scanning electron microscopy were dehydrated in amyl acetate finally. After critical-point-drying in CO_2 , they were coated with gold and examined in a Hitachi S-430 scanning electron microscope. Specimens for transmission electron microscopy were embedded in Epon 812 mixture. Thin sections were made with a diamond knife on a Sorvall Porter-Blum MT-1 microtome, stained with 3% aqueous uranyl acetate and viewed with a Hitachi HS-9 electron microscope.

RESULTS

Live spermatozoa of *Haliotis discus* are distinguishable as being composed of four structural units, a large acrosome, cylindrical nucleus, midpiece, and a long tail when observed under the Nomarski differential interference microscope (Fig. 1). The acrosome exhibits a shape like a pencil cap at the top of the sperm head. It appears to be structurally separated from the cylindrical nucleus by a constriction or a boundary with a narrow gap. Observations with a dark-field microscope also reveal that the acrosome is clearly distinguishable from the nucleus, both being seen as distinct compartments (photographs not shown). By using the Nomarski differential interference microscope, the midpiece is seen to be attached to the posterior end of the nucleus. Observations at a higher magnification indicate that the central region of the posterior half of the acrosome and of the anterior part of the nucleus can be distinguished as a light refracting streak (Fig. 1). This streak corresponds to the acrosomal and nuclear fossae observed by transmission electron microscopy.

Scanning electron micrographs reveal that the spermatozoon has a head with a length of about $6.5\text{ }\mu\text{m}$ and a tail of about $40\text{ }\mu\text{m}$ long (Fig. 2). The head of the spermatozoon is confirmed to consist of a huge acrosome, a cylindrical nucleus, and a midpiece at the posterior end of the nucleus. The tail reveals a uniform width except at the tip region that is evidently slimmer. These structural features are clearly seen in Fig. 3 at a higher magnification.

The acrosome is about $2.8\text{ }\mu\text{m}$ in length (ranging from 2.7 to $3.0\text{ }\mu\text{m}$) and $1.1\text{ }\mu\text{m}$ in diameter at the posterior part, showing a dimension nearly identical to that of the nucleus. Fig. 3 shows that by scanning electron microscopy the acrosome can be distinguished from the nucleus by a sharp neck which corresponds to the constriction seen under the Nomarski microscope (Fig. 1). Furthermore, the longitudinal section of the acrosome by transmission electron microscopy (Fig. 4) shows that the acrosomal vesicle is clearly separated from the nucleus by a definite membrane called acrosomal membrane.

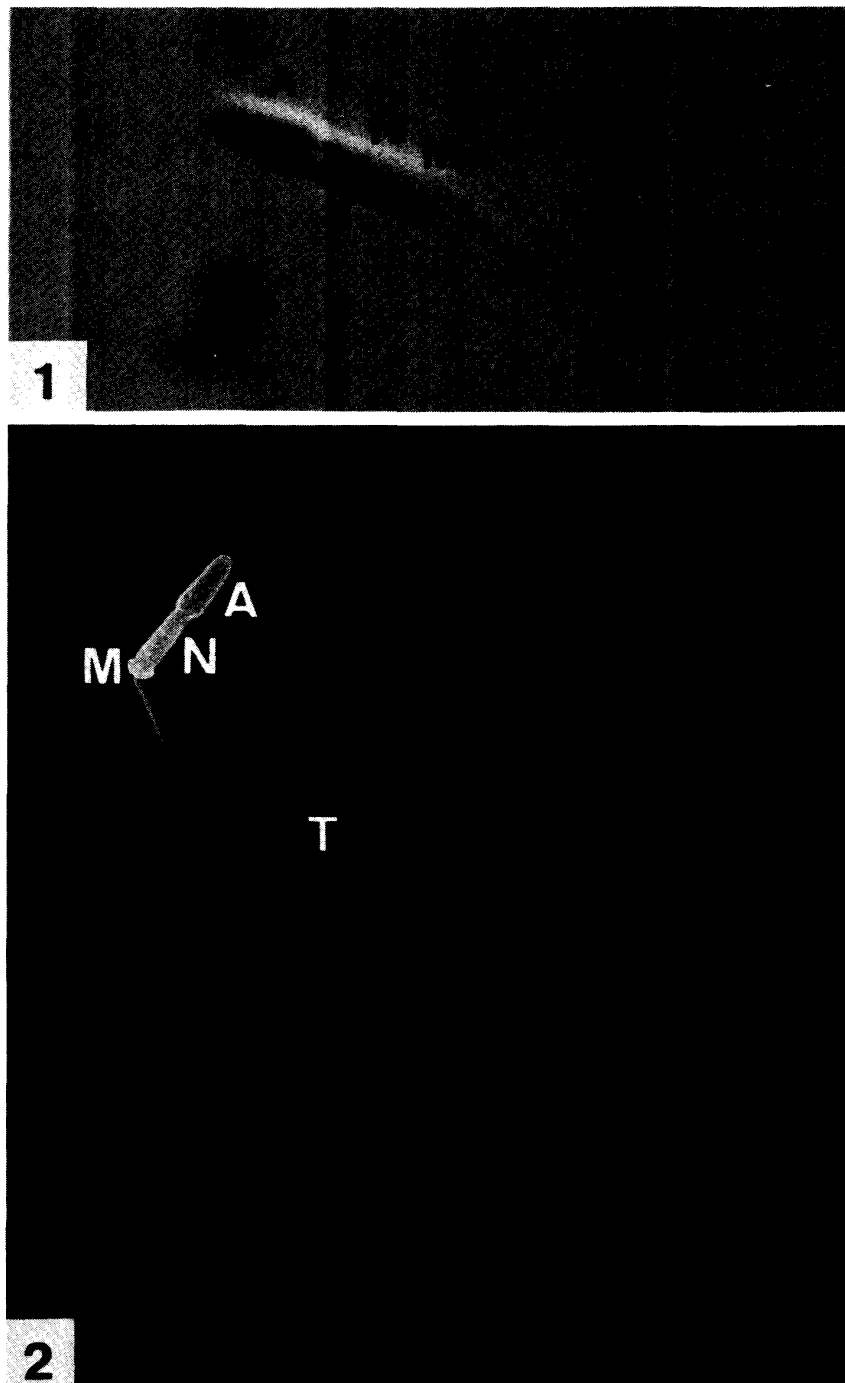
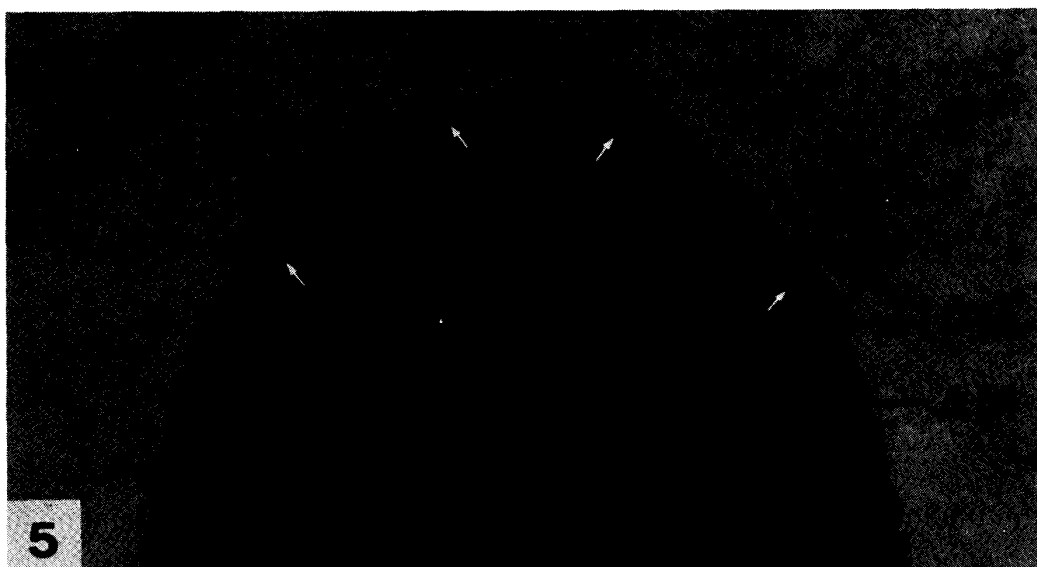
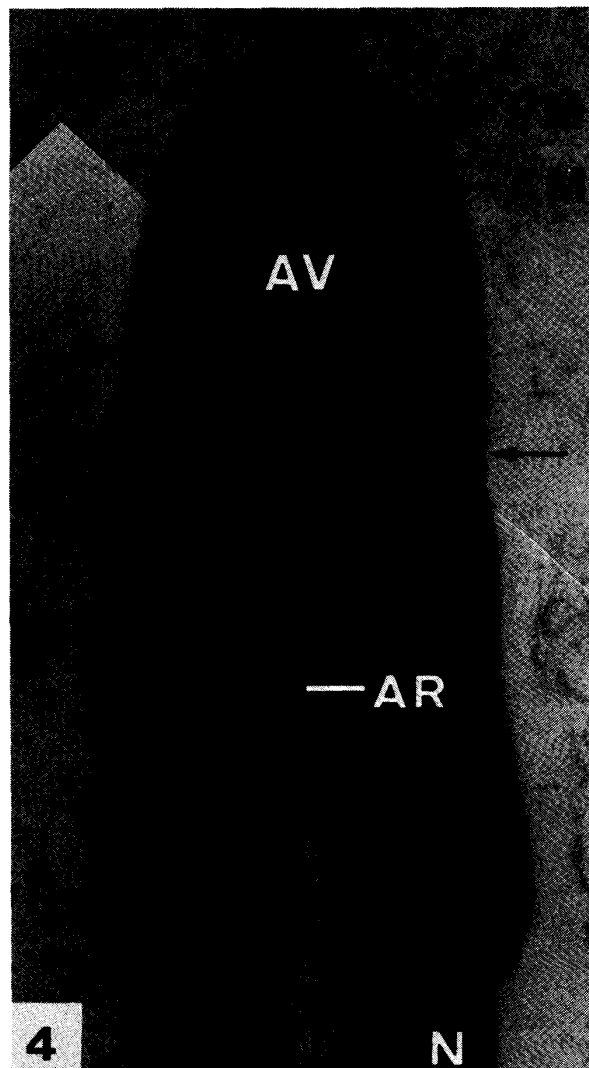
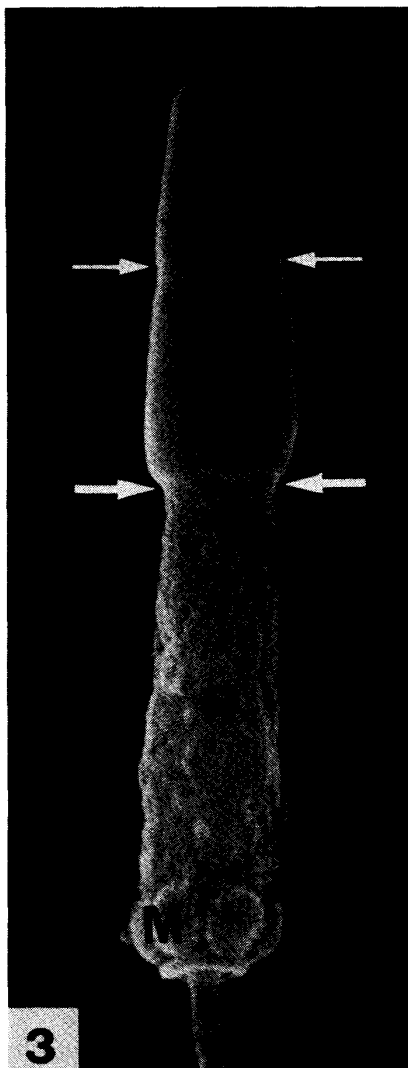


Fig. 1. Differential interference micrograph of *H. discus* spermatozoon. A, acrosome; N, nucleus; M, midpiece; T, tail. $\times 4,000$ approximately.

Fig. 2. Scanning electron micrograph of the entire *H. discus* spermatozoon. A, acrosome; N, nucleus; M, midpiece; T, tail. $\times 2,570$.



The posterior part of this acrosomal vesicle is invaginated to form a narrow blind tube extending about one-half the length of the acrosome (Fig. 4). The acrosomal vesicle itself contains two homogeneous materials different in electron density. A more electron-dense material in the anterior part adjoins the apical part of the acrosomal vesicle with its posterior boundary in contact with the apex of the invagination, and a less dense material occupies the posterior part of the acrosomal vesicle. No membrane can be detected at the boundary between these two materials in thin sections. In the scanning electron micrographs, the boundary can be clearly detected by a constriction, which is also seen in thin sections as a slight depression at the surface of the acrosome where these two materials contact (Figs. 3 and 4, arrows).

- Fig. 3. Scanning electron micrograph of the sperm head. Upper arrows point to a small constriction corresponding to the boundary between the two contents of the acrosomal vesicle. Lower arrows point to the sharp neck at the boundary of the acrosome and the nucleus with a rough surface. A, acrosome; N, nucleus; M, midpiece; T, tail. $\times 16,000$.
- Fig. 4. Longitudinal section through the acrosome. Arrows point to the constriction observed at the boundary between the electron-dense and less-dense contents of the acrosomal vesicle. AV, acrosomal vesicle; AR, axial rod; N, nucleus; PM, plasma membrane; AM, acrosomal membrane. $\times 40,000$.
- Fig. 5. Longitudinal section through the apex of the acrosome (enlarged figure of a serial section of Fig. 4). Downward arrows indicate the extent of the flat apical region where the acrosomal and plasma membranes are closely adjacent. Upward arrows indicate the electron-dense layer called the truncated cone. PM, plasma membrane; AM, acrosomal membrane. $\times 90,000$.

In the longitudinal section through the apex of the acrosome (Fig. 5), the plasma membrane is seen closely adjacent to the outer membrane of the acrosomal vesicle. Both the membranes look as though they were composed of a double membrane. However, the plasma membrane remains distinguishable from the acrosomal membrane by maintaining a uniform narrow space in between except for a flat region at the apex of the acrosomal vesicle, where the two membranes are closely apposed. Between the apposed membranes some connections are visible (Fig. 5).

Following the flat top of the acrosome, electron dense structures are observed at both sides of the anterior outer part of the acrosome, which form a wall extending down from the rim of the flat region with a thickness of about 17 to 20 nm (Fig. 5). This structure was previously called the truncated cone (7).

A bundle of fibrous material termed axial rod is contained within the invagination of the posterior part of the acrosomal vesicle (Figs. 6 and 7). The posterior part of the rod is seen to penetrate deeply into the anterior part of the nucleus forming a nuclear invagination surrounded by the nuclear envelope (Figs. 6 and 8). The compartment by these invaginations exhibits a characteristic shape. The tube expands widest at the border between the acrosomal vesicle and the nucleus, to form a diamond-shaped region, where the rod appears to be surrounded by amorphous materials (Fig. 6). The rod maintains a uniform diameter of about $0.15\ \mu\text{m}$ throughout its length within the blind tube. The neck region of the invaginated acrosomal membrane is capped by a thin electron dense layer (Fig. 6). The diamond-shaped region seems to correspond to the narrow gap between the acrosome and the nucleus observed by Nomarski microscopy (Fig. 1).

The nucleus constitutes approximately half of the sperm head. Scanning electron micrographs show that the cylindrical nucleus having a diameter of about $1.0\ \mu\text{m}$ and a length of about $2.8\ \mu\text{m}$ exhibits a rough surface in contrast with the acrosome (Fig. 3). In transmission electron micrographs, the contents of the nucleus, namely the supercondensed chromatin, are

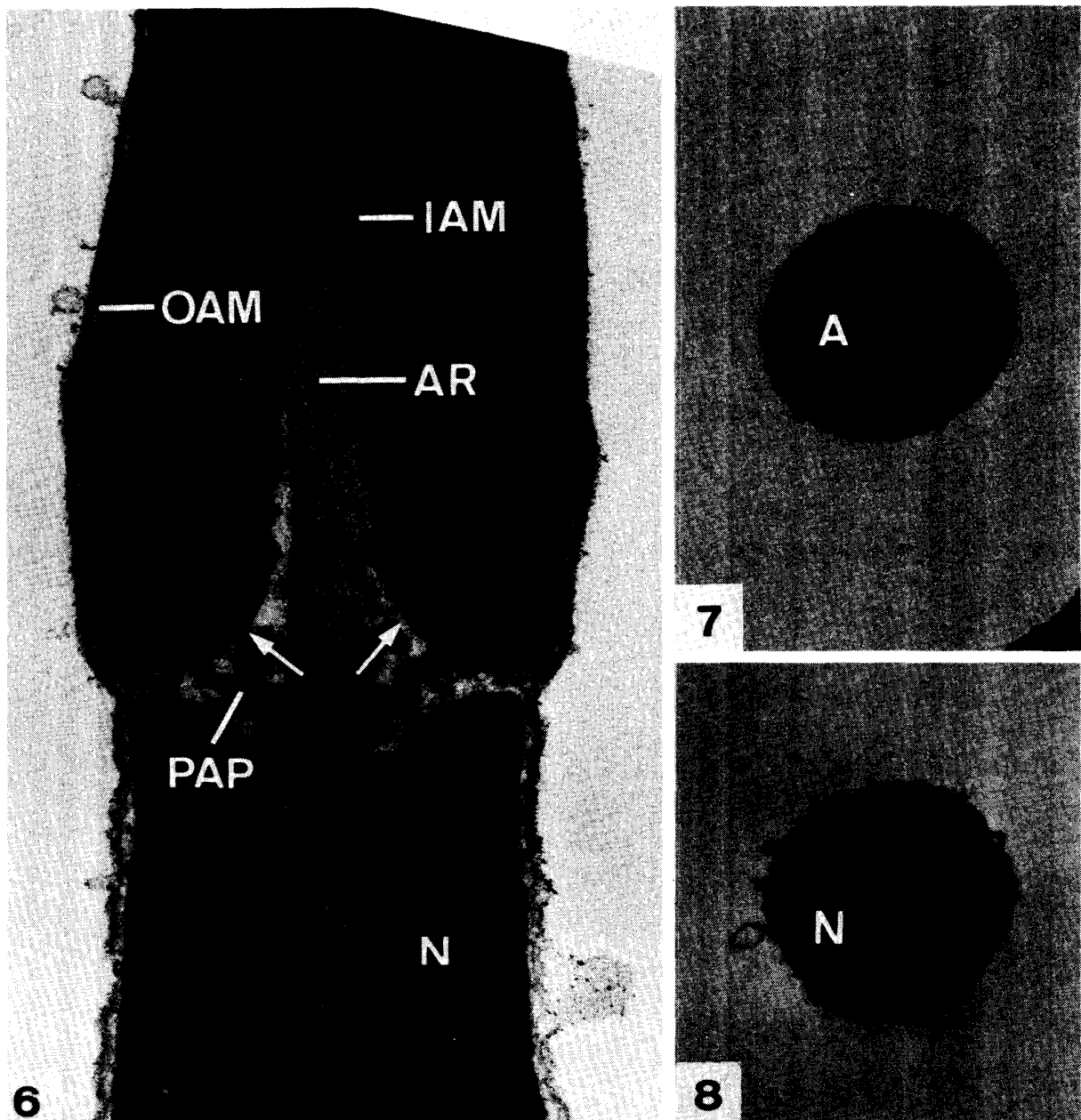
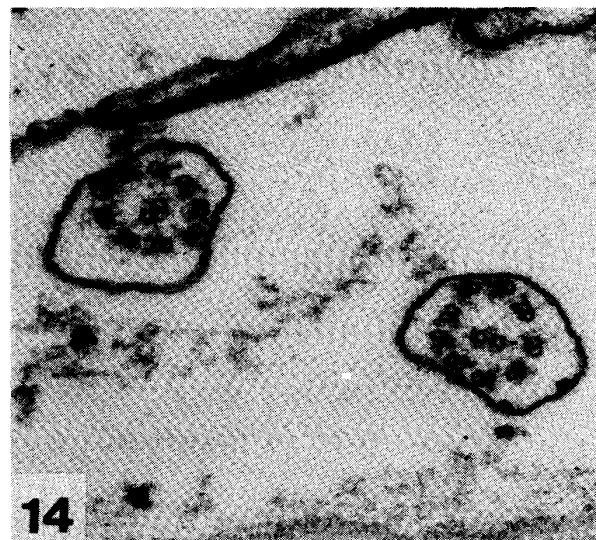
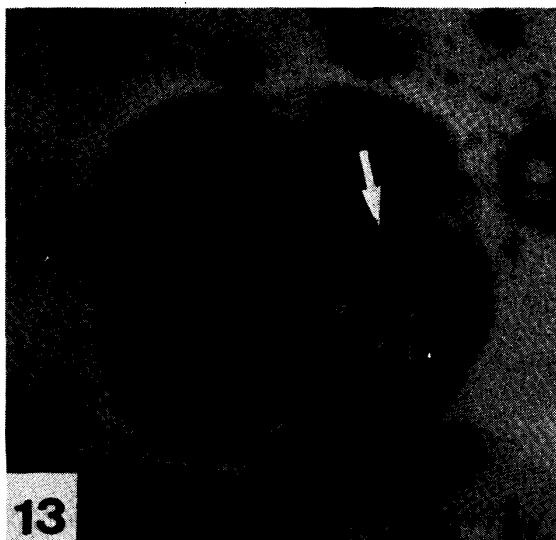
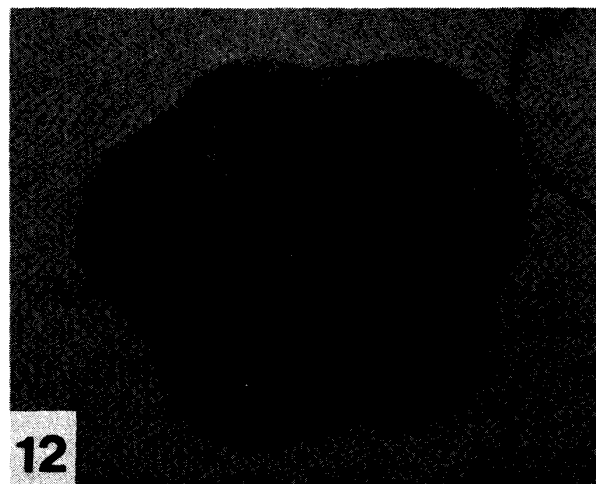
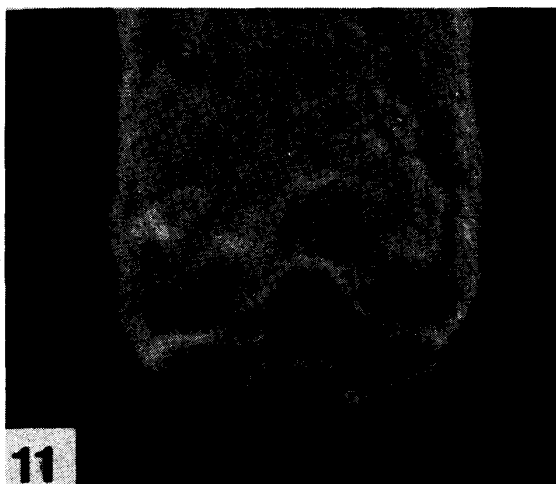
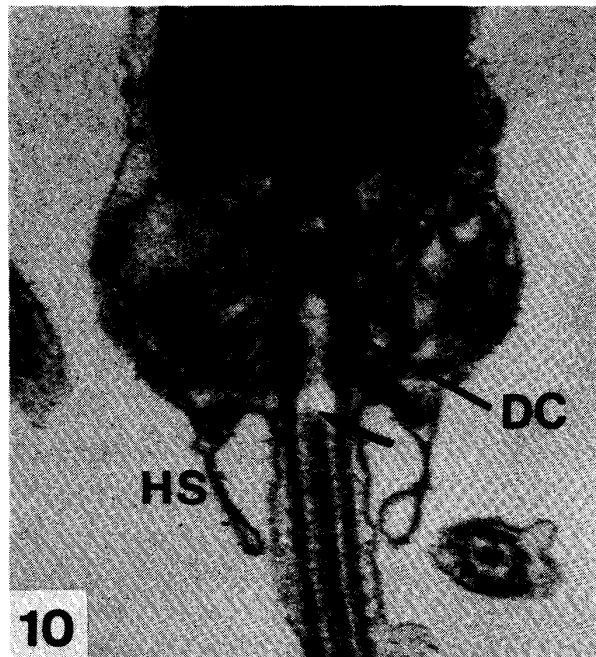
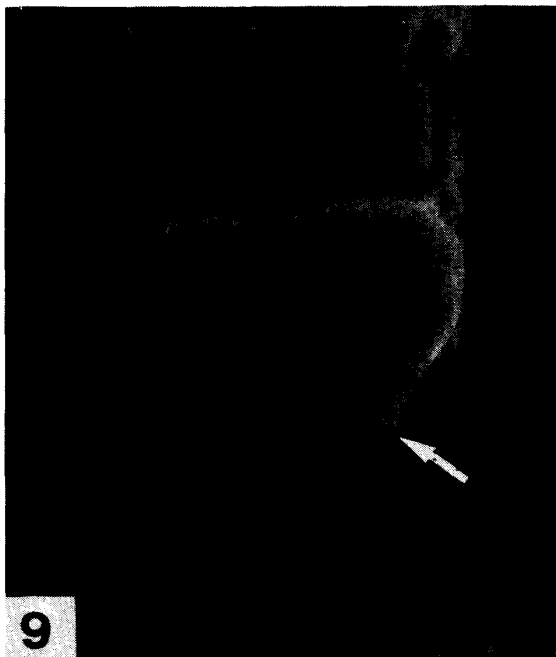


Fig. 6. Longitudinal section showing the axial rod. Arrows indicate the electron dense layer at the neck of the invaginated inner acrosomal membrane. AR, axial rod; PAP, amorphous material around the axial rod (probably precursor of the acrosomal process); N, nucleus; OAM, outer acrosomal membrane; IAM, inner acrosomal membrane. $\times 60,000$.

Fig. 7. Transverse section of acrosomal invagination. A, acrosome. $\times 30,000$.

Fig. 8. Transverse section of nuclear invagination. N, nucleus. $\times 30,000$.



seen to be more electron dense than those of the acrosome (Fig. 6).

The midpiece (approximately $1.0 \times 1.1 \mu\text{m}$) attached to the posterior end of the nucleus consists of five spherical mitochondria and a pair of centrioles from which the tail extends long (Figs. 9 and 10). The five mitochondria are arranged in a ring surrounding the centrioles (Figs. 9 and 12) and each mitochondrion makes a depression into the posterior part of the nucleus (Figs. 9 and 11). In the longitudinal sections (Fig. 10), a hook-shaped structure is observed, which hangs down from the distal border of the mitochondria, just covering the proximal end of the tail. This structure is equivalent to the flagellar sheath observed in *Oryzias* spermatozoa (9). In scanning electron micrographs (Fig. 9), this structure is observed as a ring attached to the posterior end of the five mitochondria.

Fig. 9. Scanning electron micrograph of the midpiece. Arrow shows the ring structure. Mi, mitochondria. $\times 39,000$.

Fig. 10. Longitudinal section through the midpiece. Arrow points to the proximal end of the central pair of the axoneme. HS, hook-shaped structure (compare with Fig. 9); Mi, mitochondria; PC, proximal centriole; DC, distal centriole. $\times 39,900$.

Fig. 11. Scanning electron micrograph showing the posterior surface of the nucleus from which midpiece was detached. $\times 43,000$.

Fig. 12. Transverse section through the midpiece. C, centriole; Mi, mitochondria. $\times 39,900$.

Fig. 13. Cross section through the midpiece. Arrow indicates accessory spoke. $\times 40,000$.

Fig. 14. Transverse section of the flagella. Note that a pair of flagella face opposite directions. $\times 60,000$.

A pair of centrioles termed proximal and distal centrioles are oriented orthogonally; i.e., the long axis of the proximal centriole is perpendicular to, and that of the distal one is parallel to the long axis of the sperm head (Fig. 10). The proximal centriole makes a dent at the posterior end of the nucleus. The cross section through the midpiece (Fig. 13) shows that the wall of the distal centriole is composed of nine triplets of microtubules and nine spokes connecting the centriole with the mitochondria. The tail has the 9 plus 2 structure enveloped by the plasma membrane (Figs. 10 and 14), showing nine outer doublet microtubules associated with inner and outer dynein arms which extend toward the B tubule of neighbouring doublet microtubules.

DISCUSSION

The spermatozoa of *H. discus* resembles some bivalves (3,5) and snails of mollusca in having a large size of acrosome with filamentous bundle, cylindrical nucleus and the midpiece composed of several spherical mitochondria. That the acrosome is extremely large and protruded from the nucleus allows identification even under the light microscopes. In such features, molluscan spermatozoa are quite different from those of echinoderms whose acrosome is very small and embedded in the nucleus.

Several characteristics of the *H. discus* spermatozoa observed by transmission electron microscopy are confirmed by observations of live spermatozoa under light microscopes and by scanning electron microscopy. In fact, the constriction or the narrow gap is detected between the acrosome and the nucleus as well as at the border between the nucleus and the midpiece under the Nomarski microscope. The small constriction, in addition, can be detected at the middle of the acrosome by Nomarski microscopy. The light-refracting streak is found extending in both the posterior of the acrosome and the anterior of the nucleus. This streak corresponds to the region of the axial rod observed by transmission electron

microscopy. As this region is seen more transparent than other regions under the Nomarski microscope, the refractive index of the filamentous rod should be different from that of the surrounding regions. The dark-field microscopy also favors discernment of the structural compartments in such dimension as the acrosome or the nucleus of *H. discus* spermatozoa.

As previously reported, the transmission electron micrographs indicate that the acrosome of *H. discus* is composed of two kinds of materials different in electron density each in the anterior and posterior regions (7). In the present study, the scanning electron microscopy reveals that the acrosomal vesicle is comparted into two regions by a small constriction at the middle. The longitudinal section also shows that the slight depression at the surface of the acrosome is detected at the border of the two acrosomal components. These results further confirm that the acrosomal vesicle contains at least two kinds of material. The presence of these two materials is compatible with the fact that the release of the acrosomal contents occurs in two steps during the acrosome reaction (7,10).

It should be noted here that the overall figure of the acrosome of *H. discus* quite resembles that of *H. rufescens* except that the small constriction of the acrosome was not presented in the latter (6). Neither the apex structure consisting of the closely apposed membranes of trigger region and the truncated cone, nor the capped structure of the acrosomal invagination has been reported in *H. rufescens*.

Longitudinal sections through the apex of *H. discus* acrosome reveal the closely apposed membranes covering the flat tip of the acrosome similar to the apical vesicles of the *Hydroides* and *Mytilus* spermatozoa (11,12). This locus appears to function as a trigger for initiating the acrosome reaction, since the locus was found to undergo the first structural change when the spermatozoon makes contact with the egg surface (13).

The axial rod that contains actin-like filaments is one of the characteristics in this species. This rod could be responsible for elongation of the acro-

somal process by polymerization of the sperm actin. Evidence has been presented that actin is contained in certain echinoderm spermatozoa (14). However, none of them contain such a preformed filamentous bundle. In *H. discus*, the amorphous material is found around the axial rod at the border region of the acrosomal vesicle and the nucleus, similar to the cup of amorphous material observed in *Thyone* spermatozoa (15). It could be speculated that the amorphous material in this species is transformed into filaments when the axial rod further elongates to form the acrosomal process.

The distal centriole has the accessory spokes as demonstrated in the spermatozoa of *H. rufescens* (6). In *H. discus*, however, the nine spokes are associated with each of the nine triplet microtubules as in *Oryzias* spermatozoa (9) and seem to be connected with five mitochondria. This results in four mitochondria binding to two spokes each, and one mitochondrion binding to only one spoke. This differs from the spermatozoon of *H. rufescens*, each mitochondrion being associated with two each of the 10 spokes (6).

Further studies on the structural changes of the acrosome during fertilization are now in progress.

The authors wish to thank Mr. T. Ninomiya and Mr. M. Toba of Chiba Prefectural Fisheries Experimental Station and Dr. M. Inoue and Mr. M. Chikayama of Kanagawa Prefectural Fisheries Experimental Station for providing mature abalones and for affording facilities. The authors' thanks are also due to Mr. K. Matsumoto of Nissei Sangyo Company for technical assistance in scanning electron microscopy.

REFERENCES

1. Dan, J. C. (1967) In "Fertilization. Comparative Morphology, Biochemistry, and Immunology" (Metz, C. B., and Monroy, A., eds.) Vol. 1, pp. 237-281, Academic Press, New York
2. Dan, J. C. (1975) In "Eggs and Spermatozoa" (Zool. Soc. Japan, ed.) pp. 95-97, University of Tokyo Press, Tokyo
3. Niijima, L., and Dan, J. C. (1965) J. Cell Biol. **25**, 243-248
4. Pasteels, J. J. (1965) Arch. Biol. **76**, 463-509
5. Galtsoff, P. S., and Philpott, D. E. (1960) J. Ultrastruct. Res. **3**, 241-253
6. Lewis, C. A., Leighton, D. L., and Vacquier, V. D. (1980) J. Ultrastruct. Res. **72**, 39-46
7. Sakai, Y. T., Shiroya, Y., and Haino-Fukushima, K. (1982) Develop. Growth Differ. **24**, 531-542
8. Kikuchi, S., and Uki, N. (1974) Bull. Tohoku Reg. Fish. Res. Lab. **33**, 79-86
9. Sakai, Y. T. (1976) Develop. Growth Differ. **18**, 1-13
10. Lewis, C. A., Talbot, C. F., and Vacquier, V. D. (1982) Develop. Biol. **92**, 227-239
11. Colwin, L. H., and Colwin, A. L. (1961) J. Biophys. Biochem. Cytol. **10**, 231-254
12. Dan, J. C., Kakizawa, Y., Kushida, H., and Fujita, K. (1972) Exp. Cell Res. **72**, 60-68
13. Shiroya, Y., and Sakai, Y. T. (1982) Zool. Mag. **91**, 385
14. Tilney, L. G., Hatano, S., Ishikawa, H., and Mooseker, M. S. (1973) J. Cell Biol. **59**, 109-126
15. Tilney, L. G. (1976) J. Cell Biol. **69**, 73-89